

Scalable Bayesian Nonparametric Clustering and Classification

Yang Ni¹, Peter Müller², Maurice Diesendruck¹, Sinead Williamson³, Yitan Zhu⁴, and Yuan Ji^{4,5}

¹Department of Statistics and Data Sciences, The University of Texas at Austin

²Department of Mathematics, The University of Texas at Austin

³Department of Information, Risk, and Operations Management, The University of Texas at Austin

⁴Program for Computational Genomics and Medicine, NorthShore University HealthSystem

⁵Department of Public Health Sciences, The University of Chicago

Abstract

We develop a scalable multi-step Monte Carlo algorithm for inference under a large class of nonparametric Bayesian models for clustering and classification. Each step is “embarrassingly parallel” and can be implemented using the same Markov chain Monte Carlo sampler. The simplicity and generality of our approach makes inference for a wide range of Bayesian nonparametric mixture models applicable to large datasets. Specifically, we apply the approach to inference under a product partition model with regression on covariates. We show results for inference with two motivating data sets: a large set of electronic health records (EHR) and a bank telemarketing dataset. We find interesting clusters and favorable classification performance relative to other widely used competing classifiers.

Keywords: Electronic health records, non-conjugate models, parallel computing, product partition models.

1 Introduction

We propose a distributed Monte Carlo algorithm for Bayesian nonparametric clustering and classification methods that are suitable for data with large sample size. The algorithm is applicable for both conjugate and non-conjugate structures, and consists of K computationally efficient steps. K is dynamically determined and is typically less than 4. In each of the first $(K - 1)$ steps, we divide the data into many shards and run “embarrassingly parallel” Markov chain Monte Carlo (MCMC) simulations in each shard. In the last step, MCMC is run again to generate approximate samples from the full posterior. We apply the algorithm for inference in a product partition model with regression on covariates (PPMx, Müller et al. 2011), and show results for a large electronic health records (EHR) dataset and a dataset of telemarketing for long-term bank deposits. Our method is scalable, outperforms state-of-the-art classifiers and generates interpretable partitions of the data.

Classification and clustering. We consider Bayesian nonparametric (BNP) methods for clustering and classification. Classification aims to assign observations into two or more categories on the basis of training data with known categories. Widely used classification algorithms include logistic regression (LR), naive Bayes, neural networks, k-nearest neighbors, support vector machines (SVM, Cortes and Vapnik 1995), decision trees, random forests (RF, Ho 1995), classification and regression trees (Breiman et al. 1984), Bayesian additive regression trees (BART, Chipman et al. 2010) and mixture models based on Bayesian nonparametric (BNP) priors. Some recent examples for the latter are Cruz-Mesía et al. (2007) who use a dependent Dirichlet process prior, Mansinghka et al. (2007) who model the distribution within each subpopulation defined by the class labels using a Dirichlet process mixture model, or Gutiérrez et al. (2014) who use a geometric-weights prior instead. For more examples, see a recent review by Singh et al. (2016) and references therein.

In contrast to supervised learning in classification, clustering methods partition the observations into latent groups/clusters in an unsupervised manner, with the aim of creating homogeneous groups such that observations in the same cluster are more similar to each other than to those in other clusters. Widely used clustering methods include hierarchical clustering, k-means, DBSCAN (Ester et al., 1996) and finite mixture models. Posterior simulation for finite mixtures was first discussed in Richardson and Green (1997) and extended to multivariate mixtures in Dellaportas and Papageorgiou (2006). See, for example,

Jain (2010) and Fahad et al. (2014) for recent reviews.

BNP (Hjort et al., 2010) clustering methods offer a wide range of flexible alternatives to classical clustering algorithms including Dirichlet process mixtures (DPM, (Lo, 1984; MacEachern, 2000; Lau and Green, 2007) and variations with different data structures, such as (Rodriguez et al., 2011) for a mixture of graphical models, Pitman-Yor (PY) process mixtures (Pitman and Yor, 1997; Ni et al., 2018), normalized inverse Gaussian process mixtures (Lijoi et al., 2005), normalized generalized Gamma process mixtures (Lijoi et al., 2007), and more general classes of BNP mixture models (Barrios et al., 2013; Favaro and Teh, 2013; Argiento et al., 2010).

Scalable methods. Datasets that are too large to be analyzed on a single machine increasingly occur in many applications, including health care, online streaming, social media, education, banking and finance. Many of the earlier mentioned classification or clustering methods do not scale to large datasets, partly due to lack of straightforward parallelization. Below, we briefly review some recently proposed efficient computational strategies.

Zhang et al. (2012) developed two algorithms for parallel statistical optimization based on averaging and bootstrapping. Kleiner et al. (2014) developed a scalable bootstrap to evaluate the uncertainty of estimators.

Bayesian methods naturally provide uncertainty quantification of estimators but are in general computation-intensive. Huang and Gelman (2005) proposed consensus Monte Carlo algorithms that distribute data to multiple machines running separate MCMC simulations in parallel. Various ways of eventually consolidating simulations from these subset posteriors have been proposed (Neiswanger et al., 2013; Wang and Dunson, 2013; White et al., 2015; Minsker et al., 2014; Scott et al., 2016). An alternative strategy for scalable Bayesian computation is based on approximating the full likelihood/posterior using subsampling techniques (Welling and Teh, 2011; Korattikara et al., 2014; Bardenet et al., 2014; Quiroz et al., 2018); see Bardenet et al. (2015) for a review of related recent MCMC approaches. Alternatively to MCMC, Bayesian inference can be carried out by using approximation such as variational Bayes (Jaakkola and Jordan, 2000; Ghahramani and Beal, 2001; Broderick et al., 2013; Hoffman et al., 2013). For a grand overview of Bayesian computation, see also Green et al. (2015). Although variational inference is scalable to large-scale datasets and usually yields good approximations to the marginal posterior, MCMC algorithms tend

to better approximate the joint posterior because they are simulation-exact methods.

Scalable classification and clustering. Some classical classifiers like logistic regression are scalable to large datasets and easy to interpret. However, the performance of logistic regression tends to be not as accurate as other “black box” classifiers. Ideally, a good classifier does not need to sacrifice its predictive performance for interpretability and scalability. This is what we aim to achieve in this paper.

Some work has been done in this area. Payne and Mallick (2018) developed a two-stage Metropolis-Hastings algorithm for logistic regression to avoid the need for exact likelihood computation. The first stage, based on an approximate likelihood, is used to determine whether a full likelihood evaluation is necessary in the second stage. Combined with consensus Monte Carlo, the proposed method scales well to datasets with large samples. Rebentrost et al. (2014) implemented SVM on a quantum computer and showed an exponential speed-up compared to classical sampling algorithms.

For clustering, Pennell and Dunson (2007) developed a two-stage approach for fitting random effects models to longitudinal data with large sample size. They first cluster subjects using a deterministic algorithm and then cluster the group-specific random effects using a DPM model. Zhao et al. (2009) proposed a parallel k-means clustering algorithm using the MapReduce framework (Dean and Ghemawat, 2008). Wang and Dunson (2011) developed a single-pass sequential algorithm for conjugate DPM models. In each iteration, they deterministically assign new subject to the cluster with the highest probability conditional on past cluster assignments and the data up to current observation. The algorithm is repeated for multiple permutations of the samples. Lin (2013) also proposed a one-pass sequential algorithm for DPM models. The algorithm utilizes a constructive characterization of the posterior distribution of the mixing distribution given data and partition. Variational inference is adopted to sequentially approximate the marginalization. Williamson et al. (2013) introduced a parallel MCMC for DPM models which involves iteration over local updates and a global update. For the local update, they exploit the fact that Dirichlet mixtures of Dirichlet process (DP) are DP if the parameters of Dirichlet mixture are suitably chosen. Ge et al. (2015) used a similar characterization of the DP as in Lin (2013). But instead of variational approximation, they adapted the slice sampler for parallel computing under a MapReduce framework. Tank et al. (2015) developed two variational inference algorithms for general BNP mixture models.

The method most similar to that proposed in this paper is the subset nonparametric Bayesian (SNOB) clustering of Zuanetti et al. (2018), a computation-efficient alternative for model-based clustering under a DPM model with conjugate priors. SNOB is a two-step approach. It first splits data into shards and computes the clusters locally in parallel. A second step combines the local clusters into global clusters. All steps are carried out using MCMC simulation under a common DPM model. However, the method requires conjugate models.

Proposed method. Inspired by Neal’s algorithm 8 (Neal, 2000) for inference in DPM models, we extend SNOB to clustering under non-conjugate BNP models, and propose a multi-step algorithm for subset inference of general nonparametric Bayesian methods (SIGN). The algorithm is a K -step approach (K is dynamically determined and will be introduced in Section 2.2) . Each step requires computationally intensive clustering on small subsets only. The number of required subsets is linear in the sample size n , making it possible to implement posterior inference also for data that is too large to allow the use of full MCMC simulation. SIGN can be applied with a large class of BNP mixture models. Particularly, we show how SIGN is implemented for inference under the PPMx model to simultaneously cluster and classify patients from a large Chinese EHR dataset with 85,021 samples and customers from a bank telemarketing dataset with 37,078 records.

In the context of a classification problem, SIGN still requires that all data can be accessed. This is not an inherent constraint of the proposed algorithm; rather it is due to the lack of sufficient/summary statistics for classification models (such as probit regression). Whenever such statistics exist, SIGN does not need to access the entire dataset.

The remainder of this paper is organized as follows. In Section 2.2, we introduce the proposed SIGN algorithm which is applied for inference under the PPMx model in Section 3. The SIGN algorithm is evaluated with simulation studies in Section 4 and applied to EHR and bank telemarketing data in Section 5. We conclude with a discussion in Section 6.

2 The proposed SIGN algorithm

2.1 BNP clustering

We propose an algorithm for posterior inference on random partitions under BNP mixture models. To state the general model, we need some notation. A partition $\rho = \{S_1, \dots, S_C\}$ of an index set $[n] = \{1, \dots, n\}$ is a collection of nonempty, disjoint and exhaustive subsets $S_c \subseteq [n]$. The partition can alternatively be represented by a set of cluster membership indicators $\mathbf{s} = (s_1, \dots, s_n)$ with $s_i = c$ if $i \in S_c$. Throughout the paper, we will use superscript $-i$ to represent the appropriate quantity with the i th sample or the i th item (defined later) removed. For instance, $\mathbf{s}^{-i} = \mathbf{s} \setminus s_i$ and $\rho^{-i} = (\rho \setminus S_{s_i}) \cup (S_{s_i} \setminus i)$ are the cluster memberships and partition after removing index i .

In what follows we consider a *random* partition ρ with prior probability distribution $p(\rho)$. Let $n_c = |S_c|$ denote the cardinalities of the partitioning subsets. Let $\mathbf{n} = (n_1, \dots, n_C)$ and let \mathbf{n}^{j+} denote \mathbf{n} with the j th element incremented by 1. The random partition is called exchangeable if $p(\rho) = f(\mathbf{n})$ for a symmetric (in its arguments) function $f(\mathbf{n})$ and if $f(\mathbf{n}) = \sum_{j=1}^{C+1} f(\mathbf{n}^{j+})$. The function $f(\mathbf{n})$ is known as the exchangeable partition probability function (EPPF). By Kingman's representation theorem (Kingman, 1978), any exchangeable random partition can be characterized as the groups formed by ties under i.i.d. sampling from a discrete probability measure $G = \sum_{h=1}^{\infty} w_h \delta_{m_h}$. That is, ρ is determined by the ties among $\theta_i \sim G$, $i = 1, \dots, n$. We denote the unique values of θ_i 's by $\theta_1^*, \dots, \theta_C^*$, implying $i \in S_c$ if $\theta_i = \theta_c^*$. See, for example, Lee et al. (2013) for a discussion. It follows that a prior probability model for an exchangeable random partition ρ can always be defined as a prior $p(G)$ on a random discrete distribution $G = \sum_{h=1}^{\infty} w_h \delta_{m_h}$. This implicit definition of $p(\rho)$ by a BNP prior $p(G)$ on the random probability measure G is a commonly used specification of random partition models. The construction already includes cluster-specific parameters θ_c^* which are useful for the construction of a sampling model conditional on the partition. We use it in the next step of the model construction.

The model on G and θ_i is completed with a sampling model for the observed data conditional on ρ . For example, the θ_i could index a sampling model $p(y_i | \theta_i)$, implying that all observations in a cluster share the same sampling model. In summary,

$$y_i | \theta_i \sim p(y_i | \theta_i), \quad \theta_i | G \sim G, \quad G \sim H,$$

where G is a discrete prior distribution of θ_i and H is the BNP prior for the random probability measure G .

There are a number of options for H . A popular choice is the DP, which yields an EPPF of the form $p(\rho|\mathbf{n}) \propto \alpha^{C-1} \prod_{c=1}^C (n_c - 1)!$ where α is the concentration parameter. Other choices include PY, the normalized inverse Gaussian process and the normalized generalized gamma process. In many applications, the focus is on the posterior distribution of the random partition ρ , which can be approximated by various MCMC algorithms, including, among many others, Escobar (1994), MacEachern and Müller (1998), Neal (2000) and Walker (2007), and – for more general models – Barrios et al. (2013) or Favaro and Teh (2013). However, MCMC is only practicable for small to moderate datasets. Directly applying MCMC to large datasets is very costly because the algorithm has to scan through all the observations at every iteration, each requiring likelihood and prior evaluations. We consider inference on ρ with large sample size in next section.

2.2 SIGN algorithm

The proposed SIGN algorithm proceeds in steps. For illustration, an example workflow of SIGN with $K = 3$ steps is shown in Figure 1. Importantly, across all steps of the algorithm, all updates of cluster configurations (initially of observations, and of sets of observations in later steps) are based on a single underlying BNP mixture model for the data. Details of the implied probabilities for clustering sets of observations are given later.

Step 1. In the first step, the full dataset is randomly split into $M_1 = 4$ shards; the observations from each shard are denoted by a distinct symbol in the figure. A clustering algorithm (Neal’s algorithm 8, in our case) is then applied to cluster the items (initially, in the first step, the observations) in each shard separately, and can be implemented in parallel. We refer to the estimated clusters, represented by the ellipses, as “local” clusters. These local clusters are frozen, meaning that the observations within each cluster will never be split in the subsequent steps although merging is possible.

Step 2. In the second step, the local clusters estimated from the previous step become the items to be clustered in the next step. That is, we freeze the earlier clusters, and only allow earlier clusters to combine to larger clusters. The items are again split into M_2 shards ($M_2 = 2$ in Figure 1), and are again clustered within each shard, still using the same underlying BNP mixture model. See later for a statement of the relevant probabilities to

cluster lower level clusters. At the end of the second step, the estimated clusters are again frozen as “regional” clusters.

Step 3. At the last step, all regional clusters are collected to form the items for the next, third, step. Again items are split into M_3 shards and clustered within each shard. In the example of Figure 1, $M_3 = 1$ and iteration stops. In general, iteration continues until the number of items is sufficiently small to be clustered in a single shard. Importantly, at each step one need to only scan through a small number of items (created by previous steps) instead of every observation in a large dataset.

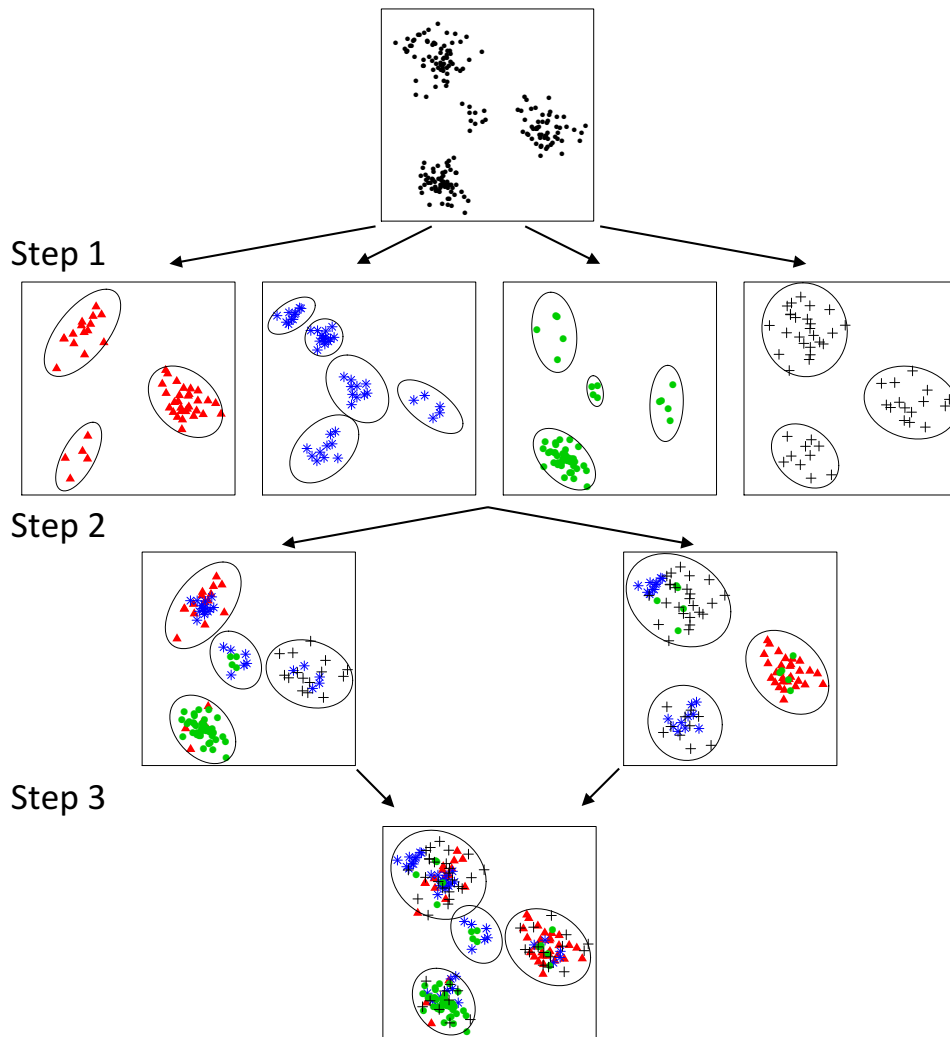


Figure 1: Example workflow of a 3-step SIGN algorithm. Step 1: the dataset is randomly distributed into 4 shards, each denoted by a unique type (color) of marker and observations are partitioned into local clusters (represented by the ellipses) within each shard in parallel. Step 2: local clusters are randomly distributed into 2 shards and partitioned into regional clusters within each shard. Step 3: regional clusters are aggregated and partitioned into global clusters.

Each step can be implemented in parallel using instances of the same MCMC algorithm which takes as input a set of (current) items, generically denoted by $\tilde{\mathbf{y}} = \{\tilde{\mathbf{y}}_1, \dots, \tilde{\mathbf{y}}_B\}$, and outputs estimated clusters of these items. Those clusters then define the items for the next step of the algorithm. Initially, in step 1, $\tilde{\mathbf{y}}_i = \mathbf{y}_i$ are the original data. Let $r_i = |\tilde{\mathbf{y}}_i|$, $i = 1, \dots, B$, denote the size of each item, in terms of number of original data that form $\tilde{\mathbf{y}}_i$, and let $\mathbf{r} = \{r_1, \dots, r_B\}$.

Posterior probabilities for clustering sets of observations. In each of the K steps, the MCMC algorithm iterates between (i) updating the cluster membership, and (ii) updating cluster-specific parameters given the cluster membership. The key quantity in updating the cluster membership is the conditional probability

$$p(\tilde{s}_i = c \mid \tilde{\mathbf{s}}^{-i}, \tilde{\mathbf{y}}, \mathbf{n}, \boldsymbol{\theta}^*) \propto p(\tilde{s}_i = c \mid \tilde{\mathbf{s}}^{-i}, \mathbf{n})p(\tilde{\mathbf{y}}_i \mid \boldsymbol{\theta}^*) \quad (1)$$

for $i = 1, \dots, B$ and $c = 1, \dots, C^{-i} + 1$ where $\tilde{s}_i = c$ means that item i is in cluster c , i.e., all observations in $\tilde{\mathbf{y}}_i$ are assigned to cluster c . The definition of the items $\tilde{\mathbf{y}}_i$ and the number of items, B , changes across steps. Initially, $\tilde{\mathbf{y}}_i$ are the original data, and $B = n$ is the sample size. In step 2, the items $\tilde{\mathbf{y}}_i$ are the local clusters and B is the total number of local clusters, etc. Importantly, the probabilities that are evaluated under (1) and used for clustering in steps 1 through 3 are all based on the same BNP mixture model for the original observations.

Equation (1) states the implied probabilities for combining clusters of observations into larger clusters. The first factor can be evaluated as

$$p(\tilde{s}_i = c \mid \tilde{\mathbf{s}}^{-i}, \mathbf{n}) \propto \frac{p(\rho^{+c} \mid \mathbf{n})}{p(\rho^{-i} \mid \mathbf{n}^{-i})} \quad (2)$$

where $\rho^{+c} = (\rho^{-i} \setminus S_c^{-i}) \cup (S_c^{-i} \cup \tilde{i})$ is the new partition that assigns the i th item to cluster c (together with all original data that make up $\tilde{\mathbf{y}}_i$). The partition probabilities on the right-hand side of (2) depend on \mathbf{r}, \mathbf{n} and the BNP prior H . For example, using $H = PY(\alpha, d, G_0)$ with concentration parameter α , discount parameter d and baseline probability measure G_0 defines the prior partition,

$$p(\rho \mid \mathbf{n}) \propto (\alpha \mid d)_C \prod_{c=1}^C (1-d)_{n_c-1}, \quad (3)$$

where $(x)_n = x(x+1)\dots(x+n-1)$ denotes the Pochhammer symbol of a rising factorial, and $(x|y)_n = x(x+y)\dots(x+(n-1)y)$ denotes the Pochhammer symbol with increment y . Substituting (3) into (2) yields

$$p(\tilde{s}_i = c \mid \tilde{\mathbf{s}}^{-i}, \mathbf{n}) \propto \begin{cases} \frac{\Gamma(n_c^{-i} + r_i - d)}{\Gamma(n_c^{-i} - d)} & \text{if } c = 1, \dots, C^{-i} \\ \frac{(\alpha + dC^{-i})\Gamma(r_i - d)}{\Gamma(1-d)} & \text{if } c = C^{-i} + 1 \end{cases}, \quad (4)$$

where n_c^{-i} is the size of the c th cluster after removing the i th item $\tilde{\mathbf{y}}_i$ (recall that size is recorded in original data units). In the special case when $r_i = |\tilde{\mathbf{y}}_i| = 1$ for all i , equation (4) reduces to the Pólya urn representation of the PY process.

The second factor in (1) is the sampling model evaluated for $\tilde{\mathbf{y}}_i$ given the cluster-specific parameters, which is straightforward to compute (see below for new empty clusters). Note that SIGN does not reduce the cost of evaluating the likelihood, however it significantly reduces the number of evaluations. The only remaining parameters to be sampled in the MCMC are the cluster-specific parameters θ_j^* . Following Algorithm 8 in Neal (2000), a value $\theta_{C^{-i}+1}^*$ for a potential new cluster is generated from the prior distribution. In the implementation, the case when resampling \tilde{s}_i removes a current cluster, say S_c , by re-assigning the only element of a singleton cluster, needs careful attention. In that case, the cluster-specific parameter θ_c^* needs to be kept for possible later use when a new cluster is considered again. At the end of each MCMC pass, we compute a least-squares estimate of the partition (Dahl, 2006). Algorithm 1 summarizes the scheme. The complete SIGN

Algorithm 1 MCMC

```

1: function MCMC( $\tilde{\mathbf{y}}$ )           //  $\tilde{\mathbf{y}} := \{\tilde{\mathbf{y}}_1, \dots, \tilde{\mathbf{y}}_B\}$ 
2:   Initialize the partition
3:   for iter = 1, ...,  $N$  do   //  $N$ : number of iterations
4:     Update cluster-specific parameters  $\theta_j^*$ 
5:     Update cluster membership,  $\tilde{s}_i$ , using (1)
6:   end for
7:   Compute the estimated partition  $\hat{\rho} = \{S_1, \dots, S_C\}$ 
8:   Output:  $\tilde{\mathbf{y}}^* = \{\tilde{\mathbf{y}}_1^*, \dots, \tilde{\mathbf{y}}_C^*\}$  //  $\tilde{\mathbf{y}}_c^* := \bigcup_{i \in S_c} \tilde{\mathbf{y}}_i$ 
9: end function

```

algorithm simply repeatedly distributes the items (i.e., blocked observations) into shards and applies Algorithm 1 to each shard in parallel. The number K of steps is dynamically determined by specifying a maximum number R (typically a few hundred) of items that can be clustered in one processor. Simulation terminates when the total number of items

is less than R . The complete scheme is summarized in Algorithm 2. SIGN implements approximate inference in the sense that the observations in the same item will not be split in any of the subsequent steps. We empirically examine the accuracy of the approximate inference compared to the full posterior inference in Section 4.

Algorithm 2 SIGN for BNP clustering

```

1: function SIGN( $\mathbf{y}, R$ )                                //  $\mathbf{y} := \{y_1, \dots, y_n\}$ 
2:   Initialize  $\tilde{\mathbf{y}} = \mathbf{y}$ 
3:   while  $B > R$  do                                    //  $B$ : number of blocks in  $\tilde{\mathbf{y}}$ 
4:     Set  $M = \lceil \frac{B}{R} \rceil$                           //  $M$ : number of shards
5:     Randomly distribute  $\tilde{\mathbf{y}}$  into  $M$  shards:  $\tilde{\mathbf{y}}_1, \dots, \tilde{\mathbf{y}}_M \subseteq \tilde{\mathbf{y}}$ 
6:     parfor each shard  $m = 1, \dots, M$  do // parallel for loop
7:        $\tilde{\mathbf{y}}_m^* = \text{MCMC}(\tilde{\mathbf{y}}_m)$                 // call Algorithm 1
8:     end parfor
9:     Set  $\tilde{\mathbf{y}} = \cup_{m=1}^M \tilde{\mathbf{y}}_m^*$  and redefine  $B$       // clusters become blocks for next step
10:  end while
11:  Output:  $\tilde{\mathbf{y}}$ 
12: end function

```

3 Clustering and classification with PPMx

The SIGN algorithm can be applied with a wide range of BNP mixture models. In this paper, we specifically consider the PPMx model that allows for simultaneously partitioning of heterogeneous samples and predicting outcomes on the basis of covariates.

To fix notation, let $z_i \in \{0, 1\}$ denote a binary outcome (reserving notation y_i for a later introduced augmented response). Let $\mathbf{x}_i = \{\mathbf{w}_i, \mathbf{u}_i\}$ denote a set of continuous covariates $\mathbf{w}_i = (w_{i1}, \dots, w_{ip})$ and a set of categorical covariates $\mathbf{u}_i = (u_{i1}, \dots, u_{iq})$ for experimental units $i = 1, \dots, n$. Let $\mathbf{z} = \{z_1, \dots, z_n\}$ and $\mathbf{x} = \{\mathbf{x}_1, \dots, \mathbf{x}_n\}$. A product partition model (PPM) (Hartigan, 1990) assumes $p(\rho) \propto \prod_{c=1}^C h(S_c)$, where $h(\cdot)$ is a non-negative cohesion function that quantifies the tightness of a cluster. For example, the prior distribution on partitions that is induced under i.i.d. sampling from a DP-distributed random measure with concentration parameter α is a PPM with $h(S_c) = \alpha \times (|S_c| - 1)!$. Müller et al. (2011) define the PPMx as a variation of the PPM by introducing prior dependence on covariates by augmenting the random partition to

$$p(\rho \mid \mathbf{x}) \propto \prod_{c=1}^C h(S_c) g(\mathbf{x}_c^*), \quad (5)$$

with a nonnegative similarity function $g(\cdot)$ indexed by covariates where $\mathbf{x}_c^* = \{\mathbf{x}_i \mid i \in S_c\}$ are the covariates of observations in the c th cluster. The similarity function measures how similar the covariates are thought to be. A computationally convenient default way to define a similarity function uses the marginal probability in an auxiliary probability model q on x :

$$g(\mathbf{x}_c^*) = \int \prod_{i \in S_c} q_x(\mathbf{x}_i \mid \boldsymbol{\xi}_c) q_\xi(\boldsymbol{\xi}_c) d\boldsymbol{\xi}_c.$$

The important feature here is that the marginal distribution has higher density value for a set of very similar x_i than for a very diverse set. For continuous covariates, we use an independent normal-normal-gamma auxiliary model, $q_x(w_{ij} \mid \mu_c, \lambda_c) = \text{N}(w_{ij} \mid \mu_c, \lambda_c^{-1})$ and $q_\xi(\mu_c, \lambda_c) = \text{N}(\mu_c \mid \mu_0, (v_0 \lambda_c)^{-1}) \times \text{Ga}(\lambda_c \mid a_\lambda, b_\lambda)$. For categorical covariates with r categories, we use a categorical-Dirichlet auxiliary model, $q_x(u_{ij} \mid \boldsymbol{\pi}_c) = \text{Cat}(u_{ij} \mid \boldsymbol{\pi}_c)$ and $q_\xi(\boldsymbol{\pi}_c) = \text{Dir}(\boldsymbol{\pi}_c \mid a_\pi, \dots, a_\pi)$ with $\boldsymbol{\pi}_c = (\pi_{c1}, \dots, \pi_{cr})$. The prior $p(\rho \mid \mathbf{x})$ introduces the desired covariate-dependent prior on the clusters S_c . Conditional on ρ we introduce cluster-specific parameters $\boldsymbol{\beta}_c$ and complete the model with a probit sampling model,

$$p(\mathbf{z} \mid \rho, \boldsymbol{\beta}, \mathbf{x}) = \prod_{c=1}^C \prod_{i \in S_c} p(z_i \mid \mathbf{x}_i, \boldsymbol{\beta}_c) = \prod_{c=1}^C \prod_{i \in S_c} p_i^{z_i} (1 - p_i)^{1-z_i} \quad (6)$$

with $p_i = \Phi(\mathbf{x}_i \boldsymbol{\beta}_c)$ and a centered multivariate normal prior on $\boldsymbol{\beta}_c \sim \text{N}(0, \tau_\beta I)$.

A practical advantage of the PPMx is its simple implementation. The posterior defined by models (5) and (6) becomes

$$p(\rho, \boldsymbol{\beta}, \boldsymbol{\xi} \mid \mathbf{z}, \mathbf{x}) \propto \prod_{c=1}^C \left[\left\{ \prod_{i \in S_c} p(z_i \mid \mathbf{x}_i, \boldsymbol{\beta}_c) q_x(\mathbf{x}_i \mid \boldsymbol{\xi}_c) \right\} p(\boldsymbol{\beta}_c) q_\xi(\boldsymbol{\xi}_c) h(S_c) \right].$$

Letting $\mathbf{y}_i = \{z_i, \mathbf{x}_i\}$, $\boldsymbol{\theta}_c^* = \{\boldsymbol{\beta}_c, \boldsymbol{\xi}_c\}$, $q_y(y_i \mid \boldsymbol{\theta}_c^*) = p(z_i \mid \mathbf{x}_i, \boldsymbol{\beta}_c) q_x(\mathbf{x}_i \mid \boldsymbol{\xi}_c)$, $q_\theta(\boldsymbol{\theta}_c^*) = p(\boldsymbol{\beta}_c) q_\xi(\boldsymbol{\xi}_c)$ and $q_\rho(\rho) = \prod_{c=1}^C h(S_c)$ one can rewrite the posterior distribution as

$$p(\rho, \boldsymbol{\beta}, \boldsymbol{\xi} \mid \mathbf{z}, \mathbf{x}) \propto \prod_{c=1}^C \prod_{i \in S_c} q_y(\mathbf{y}_i \mid \boldsymbol{\theta}_c^*) \times \prod_{c=1}^C q_\theta(\boldsymbol{\theta}_c^*) \times q_\rho(\rho). \quad (7)$$

That is, posterior inference can proceed as if \mathbf{y}_i were sampled from Equation (7). For example, in our application, we choose $q_\rho(\cdot)$ to be the random partition that is induced by a PY prior. The PY process generalizes the DP and is more flexible in modeling the number of clusters (De Blasi et al., 2015). Posterior inference under (7) can then be

carried out using Equation (1) (and hence Algorithms 1 and 2) with $p(y_i | \cdot) = q_y(y_i | \cdot)$, $H = PY(\alpha, d, G_0)$ and $G_0 = q_\theta(\cdot)$. Note how (7) is identical to the posterior in a model with data \mathbf{y}_i , cluster-specific parameters $\boldsymbol{\theta}_c^*$ and prior $q_\rho(\rho)$, allowing for easy posterior simulation.

One of the goals in our later applications is to classify a new subject, i.e., predict the binary outcome z_{n+1} , on the basis of covariates \mathbf{x}_{n+1} . It is straightforward to predict z_{n+1} using posterior averaging with respect to partitions, cluster allocation and model parameters. Let $q(\mathbf{x}_{n+1} | \mathbf{x}_c^*) = g(\mathbf{x}_c^*, \mathbf{x}_{n+1})/g(\mathbf{x}_c^*)$. The posterior predictive distribution is given by

$$p(z_{n+1} | \mathbf{x}_{n+1}, \mathbf{z}, \mathbf{x}) \propto \int \left\{ (n_c - d) \sum_{c=1}^C p(z_{n+1} | \mathbf{x}_{n+1}, \boldsymbol{\beta}_c, s_{n+1} = c) q(\mathbf{x}_{n+1} | \mathbf{x}_c^*) + (\alpha + dC) p(z_{n+1} | \mathbf{x}_{n+1}, \boldsymbol{\beta}_{C+1}) g(\mathbf{x}_{n+1}) \right\} p(\rho | \mathbf{z}, \mathbf{x}) d\rho,$$

which can be approximated by

$$p(z_{n+1} | \mathbf{x}_{n+1}, \mathbf{z}, \mathbf{x}) \propto \frac{1}{T} \sum_{t=1}^T \left\{ (n_c^{(t)} - d) \sum_{c=1}^{C^{(t)}} p(z_{n+1} | \mathbf{x}_{n+1}, \boldsymbol{\beta}_c^{(t)}, s_{n+1}^{(t)} = c) q(\mathbf{x}_{n+1} | \mathbf{x}_c^*) + (\alpha + dC^{(t)}) p(z_{n+1} | \mathbf{x}_{n+1}, \boldsymbol{\beta}_{C+1}^{(t)}) g(\mathbf{x}_{n+1}) \right\},$$

with superscript (t) indexing t th MCMC samples, $t = 1, \dots, T$, and $\boldsymbol{\beta}_{C+1}^{(t)}$ is drawn from its prior.

4 Simulation

We consider simulations with relatively small datasets with $n = 800$, $p = 5$ and $q = 5$, such that we can compare with a standard MCMC implementation of PPMx. The scalability is explored later in two case studies. We report frequentist summaries based on 50 repetitions. Throughout this section, we set the hyperparameters at $\alpha = 1$, $d = 0.5$, $\tau_\beta = 1$, $\mu_0 = 0$, $v_0 = a_\lambda = b_\lambda = 0.01$, $a_\pi = 1/r$. MCMC is run for 10,000 iterations at each step. We discard the first 50% of MCMC samples as burn-in and thin the chain by keeping every 5th sample.

4.1 Simulation I: cluster-specific probit regression

We consider a scenario where the simulation truth includes underlying clusters. In particular, we assume a simulation truth with $C_0 = 5$ clusters, and all clusters having the same size. Discrete covariates \mathbf{u}_i are generated as $u_{ij} \sim \text{Cat}(1/3, 1/3, 1/3)$, independently, $j = 1, \dots, q$. Continuous covariates \mathbf{w}_i are generated from $N_p(\boldsymbol{\mu}_c, \boldsymbol{\Sigma}_c)$ given $s_i = c$, where $\boldsymbol{\mu}_1 = (-2, 1.5, 0, 0, 0)^T$, $\boldsymbol{\mu}_2 = (0, 4, 0, 0, 0)^T$, $\boldsymbol{\mu}_3 = (0, 0, 0, 1, -2)^T$, $\boldsymbol{\mu}_4 = (1, 2, 0, 0, 0)^T$, $\boldsymbol{\mu}_5 = (0, 0, 0, -2, -2)^T$, $\boldsymbol{\Sigma}_1 = \text{diag}(0.25, 0.05^2, 1, 1, 1)$, $\boldsymbol{\Sigma}_2 = \text{diag}(1.25^2, 0.05^2, 1, 1, 1)$, $\boldsymbol{\Sigma}_3 = \text{diag}(1, 1, 1, 0.05^2, 0.25)$,

$$\boldsymbol{\Sigma}_4 = \text{blkdiag} \left(\begin{bmatrix} 0.1 & 0.05 \\ 0.05 & 0.1 \end{bmatrix}, I_3 \right) \text{ and } \boldsymbol{\Sigma}_5 = \text{blkdiag} \left(I_3, \begin{bmatrix} 0.25 & 0.125 \\ 0.125 & 0.25 \end{bmatrix} \right).$$

In words, clusters 1, 2, and 4 are characterized by a shift in the distribution for the first two continuous covariates w_{i1} and w_{i2} with different correlation structures whereas clusters 3 and 5 are characterized by a shift in the third and fourth continuous covariates w_{i4} and w_{i5} . And w_{i3} plays the role of a “noisy” covariate with the same distribution across all clusters. Covariates that do not define the clusters (such as w_{i3}, w_{i4}, w_{i5} in clusters 1, 2 and 4) are independently sampled from standard normal distributions. A typical view of the data is shown in Figure 2 where we plot w_{i1} v.s. w_{i2} and w_{i3} v.s. w_{i4} . The binary response z_i is generated from a cluster-specific probit regression, $z_i \sim \text{Bernoulli}(p_i)$ with

$$\Phi^{-1}(p_i) = \begin{cases} -1 - w_{i5} & \text{if } s_i = 1 \\ -1 + 2w_{i3} & \text{if } s_i = 2 \\ -1 + w_{i4} & \text{if } s_i = 3 \\ -1 + 1.5w_{i1} - I(u_{i1} = 2) + I(u_{i1} = 3) & \text{if } s_i = 4 \\ -1 - 1.5w_{i1} - I(u_{i2} = 2) + I(u_{i3} = 3) & \text{if } s_i = 5 \end{cases}$$

We carry out inference under the PPMx model using the default similarity functions (simply PPMx hereafter) and use a SIGN implementation with $K = 2$ steps. In the first step of SIGN, the training samples are randomly split into $M_1 = 4$ shards with each shard processing 200 samples. For comparison we also carry out inference using k-means (Hartigan and Wong, 1979) for the continuous covariates (which define the clusters) with $k = 5$ (the true number of clusters) and 20 random starting points. PPMx is always able to correctly identify the number of clusters with 5% average misclassification rate (with re-

spect to cluster assignment). SIGN selects the correct number of clusters in 48 (out of 50) simulations for which the average misclustering rate is 15%. In contrast, with k-means we find a misclassification rate of 51%.

To assess the out-of-sample predictive performance, that is, prediction of z_{n+1} , we compute the area under the ROC curve (AUC) based on 50 independent test samples generated from the same simulation truth as the training data. In addition to the comparison with PPMx, we also benchmark SIGN against four more alternative classifiers: sparse LR with lasso (R package "glmnet"), SVM ("e1071"), RF ("randomForest") and BART ("BayesTree"). For SVM, we transform the discrete covariates using dummy variables, fit with linear, cubic and Gaussian radial basis and report the best performance of the three. We grow 50,000 trees for RF and 200 trees for BART. For a fair comparison, we run BART using the same MCMC configuration as ours (i.e. 10,000 iteration, 50% burn-in and save every 5th sample). The results are reported in the first column of Table 1 where we find SIGN and PPMx have almost the same AUC's and both compare favorably with the competing classifiers.

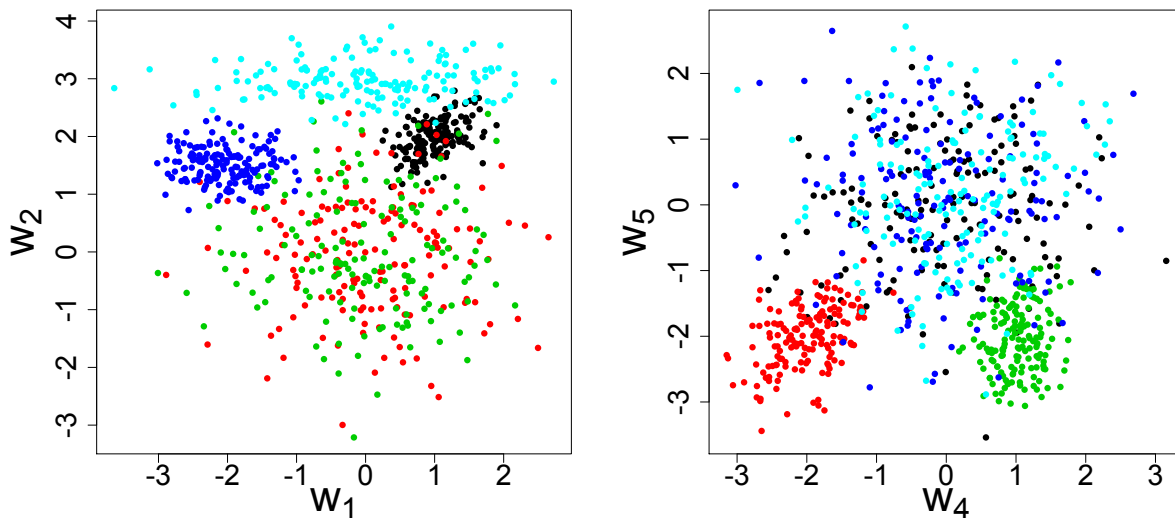


Figure 2: A typical view of data from simulation I.

4.2 Simulation II: non-linear probit regression

The favorable results for SIGN and PPMx in simulation I may be partially due to the chosen simulation truth. For an alternative comparison, in this example we use a simulation truth

different from the PPMx model. Particularly, we assume a simulation truth without an underlying clustering structure, and we generate the binary response by a nonlinear probit regression, $z_i \sim \text{Bernoulli}(p_i)$ with

$$\Phi^{-1}(p_i) = -1 + w_{i1}^2 - w_{i2}^2 + \sin(w_{i3}w_{i4}) + I(u_{i1} = 2) - I(u_{i1} = 3) - I(u_{i2} = 2) + I(u_{i2} = 3).$$

The AUC summaries for the classification are shown in the second column of Table 1. SIGN, PPMx and RF have the same AUC, $AUC = 0.84$, which is slightly lower than the AUC of BART, $AUC = 0.87$. LR and SVM do not perform well in both simulations possibly due to the parametric (linear or cubic) decision boundary in LR and the use of SVM with linear and cubic bases, and the difficulty in tuning the model parameters in SVM with radial bases.

5 Case studies

5.1 Electronic health records data: detecting diabetes

EHR data provide great opportunities as well as challenges for data-driven approaches in early disease detection. Large sample sizes allow more efficient statistical inference but at the same time impose computational challenges, especially for flexible but computation-intensive BNP models.

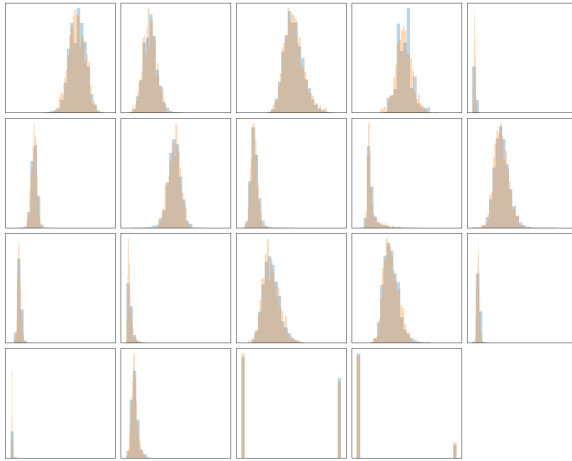
We consider EHR data for $n = 85,021$ individuals in China. The dataset is based on a physical examination of residents in some districts of a major city in China conducted in 2016. We use the data to develop a model for chronic disease prediction, specifically for diabetes. We extract data on diabetes from the items “medical history” and “other current diseases” in the physical examination form. If either of the two items of a subject contain diabetes, that subject is considered as having diabetes. We denote the diabetes status by z_i (1: diabetic and 0: normal) for subjects $i = 1, \dots, n$. Blood samples were drawn from each subject and sent to a laboratory for subsequent tests. We consider test results that are thought to be relevant to diabetes. These include white blood cell count (WBC), red blood cell count (RBC), hemoglobin (HGB), platelets (PLT), fasting blood glucose (FBG), low density lipoproteins (LDL), total cholesterol (TC), triglycerides (Trig), triketopurine (TriK), high density lipoproteins (HDL), serum creatinine (SCr), serum glutamic oxaloacetic

transaminase (SGOT) and total bilirubin (TB). We also include 5 additional covariates: gender, height, weight, blood pressure and waist. Our goal is two-fold: (1) predicting diabetes; and (2) clustering a heterogeneous population into homogeneous subpopulations.

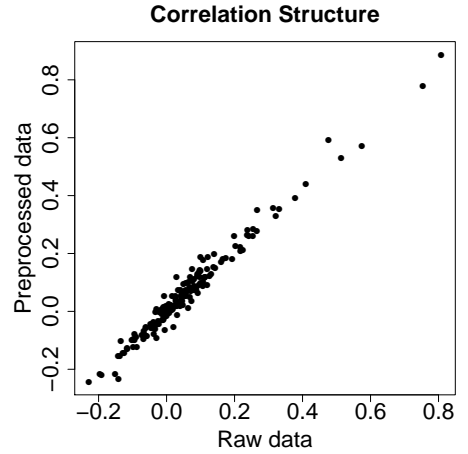
GAN preprocessing. To comply with Chinese policy, we report inference for data generated by a Generative Adversarial Network (GAN, Goodfellow et al. 2014), which replicates the distribution underlying the raw data, GAN is a machine learning algorithm which simultaneously trains a generative model and a discriminative model on a training dataset (in our case, the raw EHR dataset). The generative model simulates the training data distribution in order to trick the discriminative model. Meanwhile, the discriminative model learns to optimally distinguish between data and simulations. During training, the generative model uses gradient information from the discriminative model to produce better simulations. After training, the generative model can be used to generate an arbitrary number of simulations which are similar in distribution to the original dataset. In our case, we generate a simulated dataset of the same size as the raw EHR dataset.

For this application, we train on a dataset where columns of continuous variables are standardized, and corresponding output are then re-scaled at simulation time. To accommodate binary variables, we allow the GAN to simulate continuous values, and round corresponding outputs to 0 or 1. We use the architecture of MMD-GAN (Li et al., 2017), which uses the maximum mean discrepancy (MMD, Gretton et al., 2012), a distributional distance, to compare real data and simulations. Our implementation uses encoder and decoder networks each containing three layers of 100 nodes, connected by a bottleneck layer of 64 nodes, and with exponential linear unit activations. In our optimization, we use RMSProp with a learning rate of 0.001, and we weight the MMD in our discriminator loss function by 0.1.

Our model reaches a stable point, where both marginal distributions and pairwise correlations agree with the raw data (see Figure 3). Moreover, the classifiers we consider have similar prediction performance on the two datasets. Therefore, we only report the results based on the replicated EHR data (referred to as EHR data hereafter). To the extent to which the preprocessed data set retains all information and structure of the original data, any inference other than subject-specific summaries remains practically unchanged. See the Appendix for more details.



(a) Marginal distributions



(b) Pairwise correlations

Figure 3: GAN-preprocessed EHR data versus raw EHR data. (a) Marginal distribution of each variable. For each variable, the two overlaid histograms show the agreement between the preprocessed and the raw data. The variable names and ranges are deliberately not shown. (b) Correlation of each pair of variables. Each dot represents the Pearson correlation coefficients of one pair of variables in the raw EHR data (x-axis) versus in the GAN-preprocessed EHR data (y-axis). In total, we have $\binom{19}{2}$ pairs/dots.

Results. We randomly sample 84,750 subjects as training data and use the remaining 271 subjects as test data to evaluate out-of-sample classification performance. We implement inference under the PPMx model using the proposed SIGN algorithm. In the implementation, we use 250 compute cores (equivalent to 11 compute nodes with 24 cores per node) at the Texas Advanced Computing Center (TACC, <http://www.tacc.utexas.edu>) for computation. In the first step, the training samples are randomly split into those $M_1 = 250$ compute cores/shards with 339 samples on each shard. Collectively, we obtain 1351 local clusters. In the second step, the 1351 local clusters are distributed to $M_2 = 5$ shards with each shard taking about 270 items. The local clusters are grouped into 25 regional clusters. Iteration stops there since 25 items need not be further split, i.e., $K = 3$. In a final step, the 25 regional clusters are merged to 5 global clusters with sizes 26892, 26453, 18778, 11474 and 1153.

The AUC summaries based on the test dataset are provided in Table 1. SIGN reports the highest AUC (0.880) followed by RF and BART. As expected, the most important covariate for predicting diabetes is FBG. Regressing on FBG alone achieves $AUC = 0.829$.

Table 1: Performance of the methods used for Simulations I and II, and the two case studies. The table reports AUC for inference under SIGN, (standard implementation of) PPMx, BART, RF, LR and SVM. Numerical errors (as standard deviations over repeat simulation) are given within the parentheses.

	Simulation I	Simulation II	EHR	Bank
SIGN	0.808 (0.067)	0.838 (0.067)	0.880	0.825
PPMx	0.824 (0.060)	0.841 (0.063)	-	-
BART	0.755 (0.062)	0.866 (0.050)	0.867	0.792
RF	0.793 (0.059)	0.838 (0.067)	0.869	0.786
LR	0.600 (0.091)	0.524 (0.073)	0.856	0.781
SVM	0.622 (0.077)	0.585 (0.077)	0.856	0.761

In terms of computation time, SIGN, BART, RF and SVM take 0.9, 18.7, 3.5 and 2.5 hours with 2.6 GHz Xeon E5-2690 v3 CPU, respectively, whereas LR is several magnitude faster at the price of accuracy. We do not implement PPMx with standard MCMC, as this is not feasible with the large sample size. The good performance of SIGN may be explained by its ability to explicitly accommodate the heterogeneous nature of the subject population and allow for cluster-specific probit models in each subpopulation while leveraging model averaging to classify new subjects. For example, the estimated intercept is -1.5 for cluster 2 and -0.95 for cluster 4. The coefficient of the important covariate FBG also exhibits heterogeneity, 0.97 for cluster 3 and 0.76 for cluster 4.

5.2 Predicting the success of telemarketing

Direct marketing is a form of advertising where the salesperson directly communicates with the customers to promote business. In 2011, marketers are estimated to have spent \$163 billion on direct marketing which accounted for 52.1% of total US advertising expenditures in that year (Direct Marketing Association INC., 2012). A common direct marketing practice is by phone, known as telemarketing. In this study, we focus on predicting the success of telemarketing in selling long-term bank deposits.

We analyze a dataset collected from a Portuguese retail bank (Moro et al., 2014) with $n = 41,188$ records. The outcome of interest is whether the customer eventually subscribed a long-term deposit: $z_i = 1$ if yes, and $z_i = 0$ otherwise, $i = 1, \dots, n$. Associated with each record/customer are 20 covariates which are listed in Table 2. We follow Moro et al. (2014) and remove the covariate “last contact duration”, since the duration is unknown

Table 2: 20 Covariates in the long-term deposit data. For categorical covariates, the number within the parentheses indicates the number of categories.

Covariate name	Type
Type of job	Categorical (12)
Marital status	Categorical (4)
Education	Categorical (8)
Default or not	Categorical (3)
Housing loan or not	Categorical (3)
Contact communication type	Categorical (2)
Last contact month of year	Categorical (12)
Last contact day of the week	Categorical (5)
Outcome of the previous campaign	Categorical (3)
Age	Continuous
Last contact duration	Continuous
Number of contacts	Continuous
Number of days from a previous campaign	Continuous
Number of contacts before this campaign	Continuous
Employment variation rate	Continuous
Consumer price index	Continuous
Consumer confidence index	Continuous
Euribor 3 month rate	Continuous
Number of employees	Continuous

before a call is performed and therefore can not be used to predict the outcome of the next customer. After removing records that are inconsistent with the data description, the resulting dataset contains 37,078 records. We randomly sample $n = 36,750$ as training data and use the remaining 328 for testing purpose. Similarly to the analysis in Section 5.1, we apply PPMx using SIGN with $K = 3$ steps. In the first step, we randomly split the training data into $M_1 = 150$ shards (distributed on 7 compute nodes) with each shard taking 245 samples. We find 1,474 local clusters in the first step. Then the 1,474 local clusters are split to $M_2 = 5$ shards with each shard processing about 295 blocks of customers. In this step, the local clusters are merged into 64 regional clusters. Finally, the 64 regional clusters are grouped into 14 global clusters with cluster sizes 7,687, 6,042, 5,725, 5,130, 3,950, 2,815, 2,101, 1,484, 975, 689, 56, 48, 26 and 22.

The classification performance evaluated on the testing dataset is reported in the last column of Table 1 for SIGN, BART, RF, LR and SVM. We find SIGN outperforms all other methods with $AUC = 0.825$. The second best algorithm is BART with $AUC = 0.792$.

6 Discussion

We have introduced SIGN as a scalable algorithm for inference on clustering under BNP mixture models. SIGN can be thought of as a parallelizable extension of Neal’s algorithm 8 which is applicable to both conjugate and non-conjugate models. We use SIGN to implement inference under a PPMx model for a Chinese EHR dataset with 85,021 individuals and a bank telemarketing dataset with 37,078 customers. We find good classification performance compared with the state-of-the-art competing methods. For the EHR study, we find five meaningful clusters in the study population. We anticipate that this study will continue to collect many more subjects over the coming years. The use of algorithms that are scalable to millions of observations in terms of both computing time and memory is therefore imperative. The computing time for the proposed algorithm remains practicable with increasing sample size as long as enough computing resources are available. For example, with 1,000,000 observations, we roughly need to run SIGN for about 1 hour on 2,000 cores or equivalently around 80 compute nodes. This is feasible on many high performance computing centers such as TACC. And memory is a lesser issue because if needed one can use one large-memory compute node (192GB on TACC) in the last step where we have to access the entire dataset.

In this paper, we only consider “large n , small p ” problems. The two motivating applications include only $p = 18$ and $p = 19$ covariates. Extension to “large n , large p ” problems is of high methodological and practical interest for other problems. Another limitation of inference for the PPMx model with the current SIGN implementation is the need to access the entire dataset in the last step, which becomes computationally prohibitive for big n or p . One possible strategy is to replace the cluster-specific probit model by a simpler cluster-specific Bernoulli model for the binary response. The desired dependence between response and covariate is introduced marginally, after marginalizing with respect to the partition. Under this construction the algorithm depends on the data only through low dimensional summary statistics and could handle arbitrarily large data. A similar strategy was explored in Zuanetti et al. (2018). However, introducing the dependence between response and covariates through the partition only, we find less favorable classification performance than in the current implementations (results not shown).

Acknowledgment

Yang Ni, Peter Müller and Yuan Ji’s research were partially supported by NIH/NCI grant a R01 CA 132897. Maurice Diesendruck and Sinead Williamson were partially supported by NSF IIS-1447721. The authors acknowledge the TACC at The University of Texas at Austin for providing high performance computing resources that have contributed to the research results reported within this paper.

Appendix: GAN preprocessing details

To evaluate the privacy of the simulated set, we measure two types of risk: presence disclosure and attribute disclosure (Choi et al., 2017). Presence disclosure is the ability to determine whether a candidate point was included in the training dataset. Attribute disclosure is the ability to predict other attributes of a candidate point, given partial information about that point. For both settings, we choose three sets of equal size – 5% of the training data, a heldout set for testing, and a heldout set for baseline comparison – then estimate the sensitivity and precision of classification schemes.

For presence disclosure, we sample a candidate from the union of training and testing sets, and classify whether the candidate was included in the training set based on the presence of an ϵ -close neighbor in the simulated set. For large ϵ , the notion of ϵ -closeness is not informative, since many points are returned as neighbors, and precision scores hover around 50% – no better than random guessing. For small ϵ , few points are returned as neighbors, and neighbors are more likely to be correctly guessed, since the requirement is for a neighbor to be nearly identical to the candidate point. To reflect the optimal privacy standard, we report scores using the largest ϵ for which precision exceeds 55%. This yields the largest sensitivity under non-trivial risk, where a higher sensitivity indicates greater ability to identify a participant. At $\epsilon = 9.5$, the sensitivity of this classification is 0.0005, indicating that compromised training points would be identifiable only 0.05% of the time.

For attribute disclosure, we sample as above, and classify whether unknown features of a candidate point can be correctly estimated to within 5% of the true value, by averaging each feature over the candidate’s five nearest neighbors in the simulated set. We report values for the case in which half of the candidate’s features are known, and the other half are imputed, and note that performance did not change significantly when the percentage

of known values differed. The sensitivity and precision scores of this classification are 0.31 and 0.72, respectively, indicating that unknown features would be correctly guessed 31% of the time, and features claiming to be within 5% of the true value would in fact be 72% of the time.

We note that privacy and accuracy goals are inherently opposed. An increase in privacy corresponds to a simulated set with less information about individual data points, and vice versa. As a general guideline, we aim to satisfy privacy requirements while preserving as much as possible the utility of the simulations. In the specific case of attribute risk, we recognize that scores depend on the correlation structure of the data, where highly correlated features are more susceptible to attribute disclosure. As a baseline, we compared attribute risk scores of simulations to those of the final heldout set, and found that both were approximately 30% and 70%, respectively.

References

- Argiento, R., Guglielmi, A., and Pievatolo, A. (2010). Bayesian density estimation and model selection using nonparametric hierarchical mixtures. *Computational Statistics & Data Analysis*, 54(4):816 – 832.
- Bardenet, R., Doucet, A., and Holmes, C. (2014). Towards scaling up Markov chain Monte Carlo: an adaptive subsampling approach. In *Proceedings of the 31st International Conference on Machine Learning*, pages 405–413.
- Bardenet, R., Doucet, A., and Holmes, C. (2015). On Markov chain Monte Carlo methods for tall data. *arXiv preprint arXiv:1505.02827*.
- Barrios, E., Lijoi, A., Nieto-Barajas, L. E., and Prünster, I. (2013). Modeling with normalized random measure mixture models. *Statist. Sci.*, 28(3):313–334.
- Breiman, L., Friedman, J., Stone, C. J., and Olshen, R. A. (1984). *Classification and regression trees*. Wadsworth, Belmont, CA.
- Broderick, T., Boyd, N., Wibisono, A., Wilson, A. C., and Jordan, M. I. (2013). Streaming variational Bayes. In *Advances in Neural Information Processing Systems*, pages 1727–1735.

- Chipman, H. A., George, E. I., McCulloch, R. E., et al. (2010). BART: Bayesian additive regression trees. *The Annals of Applied Statistics*, 4(1):266–298.
- Choi, E., Biswal, S., Malin, B., Duke, J., Stewart, W. F., and Sun, J. (2017). Generating multi-label discrete patient records using generative adversarial networks. In *Proceedings of the 2nd Machine Learning for Healthcare Conference*, pages 286–305.
- Cortes, C. and Vapnik, V. (1995). Support-vector networks. *Machine Learning*, 20(3):273–297.
- Cruz-Mesía, R. D. I., Quintana, F. A., and Müller, P. (2007). Semiparametric Bayesian classification with longitudinal markers. *Journal of the Royal Statistical Society: Series C*, 56(2):119–137.
- Dahl, D. B. (2006). Model-based clustering for expression data via a Dirichlet process mixture model. *Bayesian Inference for Gene Expression and Proteomics*, pages 201–218.
- De Blasi, P., Favaro, S., Lijoi, A., Mena, R. H., Prünster, I., and Ruggiero, M. (2015). Are Gibbs-type priors the most natural generalization of the Dirichlet process? *IEEE Transactions on Pattern Analysis and Machine Intelligence*, 37(2):212–229.
- Dean, J. and Ghemawat, S. (2008). MapReduce: simplified data processing on large clusters. *Communications of the ACM*, 51(1):107–113.
- Dellaportas, P. and Papageorgiou, I. (2006). Multivariate mixtures of normals with unknown number of components. *Statistics and Computing*, 16(1):57–68.
- Direct Marketing Association INC. (2012). The power of direct marketing: ROI, sales, expenditures and employment in the US, 2011–2012. *Direct Marketing Association, Washington, DC*.
- Escobar, M. D. (1994). Estimating normal means with a Dirichlet process prior. *Journal of the American Statistical Association*, 89(425):268–277.
- Ester, M., Kriegel, H.-P., Sander, J., Xu, X., et al. (1996). A density-based algorithm for discovering clusters in large spatial databases with noise. In *KDD*, pages 226–231.

- Fahad, A., Alshatri, N., Tari, Z., Alamri, A., Khalil, I., Zomaya, A. Y., Foufou, S., and Bouras, A. (2014). A survey of clustering algorithms for big data: Taxonomy and empirical analysis. *IEEE Transactions on Emerging Topics in Computing*, 2(3):267–279.
- Favaro, S. and Teh, Y. W. (2013). MCMC for normalized random measure mixture models. *Statist. Sci.*, 28(3):335–359.
- Ge, H., Chen, Y., Wan, M., and Ghahramani, Z. (2015). Distributed inference for Dirichlet process mixture models. In *Proceedings of the 32nd International Conference on Machine Learning*, pages 2276–2284.
- Ghahramani, Z. and Beal, M. J. (2001). Propagation algorithms for variational Bayesian learning. In *Advances in Neural Information Processing Systems*, pages 507–513.
- Goodfellow, I., Pouget-Abadie, J., Mirza, M., Xu, B., Warde-Farley, D., Ozair, S., Courville, A., and Bengio, Y. (2014). Generative adversarial nets. In *Advances in Neural Information Processing Systems*, pages 2672–2680.
- Green, P. J., Łatuszyński, K., Pereyra, M., and Robert, C. P. (2015). Bayesian computation: a perspective on the current state, and sampling backwards and forwards. *arXiv preprint arXiv:1502.01148*.
- Gretton, A., Borgwardt, K. M., Rasch, M. J., Schölkopf, B., and Smola, A. (2012). A kernel two-sample test. *Journal of Machine Learning Research*, 13:723–773.
- Gutiérrez, L., Gutiérrez-Peña, E., and Mena, R. H. (2014). Bayesian nonparametric classification for spectroscopy data. *Computational Statistics & Data Analysis*, 78:56–68.
- Hartigan, J. A. (1990). Partition models. *Communications in Statistics*, 19(8):2745–2756.
- Hartigan, J. A. and Wong, M. A. (1979). Algorithm as 136: A k-means clustering algorithm. *Journal of the Royal Statistical Society. Series C*, 28(1):100–108.
- Hjort, N. L., Holmes, C., Müller, P., and Walker, S. G. (2010). *Bayesian Nonparametrics*. Cambridge Series in Statistical and Probabilistic Mathematics. Cambridge University Press, Cambridge.
- Ho, T. K. (1995). Random decision forests. In *Proceedings of the Third International Conference on Document Analysis and Recognition*, pages 278–282.

- Hoffman, M. D., Blei, D. M., Wang, C., and Paisley, J. (2013). Stochastic variational inference. *The Journal of Machine Learning Research*, 14(1):1303–1347.
- Huang, Z. and Gelman, A. (2005). Sampling for Bayesian computation with large datasets. *Technical report, Department of Statistics, Columbia University*.
- Jaakkola, T. S. and Jordan, M. I. (2000). Bayesian parameter estimation via variational methods. *Statistics and Computing*, 10(1):25–37.
- Jain, A. K. (2010). Data clustering: 50 years beyond k-means. *Pattern Recognition Letters*, 31(8):651–666.
- Kingman, J. F. C. (1978). The representation of partition structures. *Journal of the London Mathematical Society*, s2-18(2):374–380.
- Kleiner, A., Talwalkar, A., Sarkar, P., and Jordan, M. I. (2014). A scalable bootstrap for massive data. *Journal of the Royal Statistical Society: Series B*, 76(4):795–816.
- Korattikara, A., Chen, Y., and Welling, M. (2014). Austerity in MCMC land: Cutting the Metropolis-Hastings budget. In *Proceedings of the 31st International Conference on Machine Learning*, pages 181–189.
- Lau, J. W. and Green, P. J. (2007). Bayesian model-based clustering procedures. *Journal of Computational and Graphical Statistics*, 16(3):526–558.
- Lee, J., Quintana, F. A., Mülller, P., and Trippa, L. (2013). Defining predictive probability functions for species sampling models. *Statistical Science*, 28(2):209–222.
- Li, C.-L., Chang, W.-C., Cheng, Y., Yang, Y., and Póczos, B. (2017). MMD GAN: Towards deeper understanding of moment matching network. In *Advances in Neural Information Processing Systems*, pages 2200–2210.
- Lijoi, A., Mena, R. H., and Prünster, I. (2005). Hierarchical mixture modeling with normalized inverse-Gaussian priors. *Journal of the American Statistical Association*, 100(472):1278–1291.
- Lijoi, A., Mena, R. H., and Prünster, I. (2007). Controlling the reinforcement in Bayesian non-parametric mixture models. *Journal of the Royal Statistical Society: Series B*, 69(4):715–740.

- Lin, D. (2013). Online learning of nonparametric mixture models via sequential variational approximation. In *Advances in Neural Information Processing Systems*, pages 395–403.
- Lo, A. Y. (1984). On a class of Bayesian nonparametric estimates: I. Density estimates. *The Annals of Statistics*, 12(1):351–357.
- MacEachern, S. N. (2000). Dependent Dirichlet processes. *Unpublished manuscript, Department of Statistics, The Ohio State University*, pages 1–40.
- MacEachern, S. N. and Müller, P. (1998). Estimating mixture of Dirichlet process models. *Journal of Computational and Graphical Statistics*, 7(2):223–238.
- Mansinghka, V. K., Roy, D. M., Rifkin, R., and Tenenbaum, J. (2007). AClass: An online algorithm for generative classification. In *Proceedings of the 11th International Conference on Artificial Intelligence and Statistics*, pages 315–322.
- Minsker, S., Srivastava, S., Lin, L., and Dunson, D. (2014). Scalable and robust Bayesian inference via the median posterior. In *International Conference on Machine Learning*, pages 1656–1664.
- Moro, S., Cortez, P., and Rita, P. (2014). A data-driven approach to predict the success of bank telemarketing. *Decision Support Systems*, 62:22–31.
- Müller, P., Quintana, F., and Rosner, G. L. (2011). A product partition model with regression on covariates. *Journal of Computational and Graphical Statistics*, 20(1):260–278.
- Neal, R. M. (2000). Markov chain sampling methods for Dirichlet process mixture models. *Journal of Computational and Graphical Statistics*, 9(2):249–265.
- Neiswanger, W., Wang, C., and Xing, E. (2013). Asymptotically exact, embarrassingly parallel MCMC. *arXiv preprint arXiv:1311.4780*.
- Ni, Y., Müller, P., Zhu, Y., and Ji, Y. (2018). Heterogeneous reciprocal graphical models. *Biometrics*, just accepted.
- Payne, R. D. and Mallick, B. K. (2018). Two-stage Metropolis-Hastings for tall data. *Journal of Classification*, just accepted.

- Pennell, M. L. and Dunson, D. B. (2007). Fitting semiparametric random effects models to large data sets. *Biostatistics*, 8(4):821–834.
- Pitman, J. and Yor, M. (1997). The two-parameter Poisson-Dirichlet distribution derived from a stable subordinator. *The Annals of Probability*, pages 855–900.
- Quiroz, M., Kohn, R., Villani, M., and Tran, M.-N. (2018). Speeding up MCMC by efficient data subsampling. *Journal of the American Statistical Association*, (just-accepted):1–35.
- Rebentrost, P., Mohseni, M., and Lloyd, S. (2014). Quantum support vector machine for big data classification. *Physical Review Letters*, 113(13):130503.
- Richardson, S. and Green, P. J. (1997). On Bayesian analysis of mixtures with an unknown number of components (with discussion). *Journal of the Royal Statistical Society: series B*, 59(4):731–792.
- Rodriguez, A., Lenkoski, A., and Dobra, A. (2011). Sparse covariance estimation in heterogeneous samples. *Electronic Journal of Statistics*, 5:981.
- Scott, S. L., Blocker, A. W., Bonassi, F. V., Chipman, H. A., George, E. I., and McCulloch, R. E. (2016). Bayes and big data: The consensus Monte Carlo algorithm. *International Journal of Management Science and Engineering Management*, 11(2):78–88.
- Singh, A., Thakur, N., and Sharma, A. (2016). A review of supervised machine learning algorithms. In *Computing for Sustainable Global Development (INDIACom), 2016 3rd International Conference on*, pages 1310–1315. IEEE.
- Tank, A., Foti, N., and Fox, E. (2015). Streaming variational inference for Bayesian non-parametric mixture models. In *Proceedings of the Eighteenth International Conference on Artificial Intelligence and Statistics*, pages 968–976.
- Walker, S. G. (2007). Sampling the Dirichlet mixture model with slices. *Communications in Statistics*, 36(1):45–54.
- Wang, L. and Dunson, D. B. (2011). Fast Bayesian inference in Dirichlet process mixture models. *Journal of Computational and Graphical Statistics*, 20(1):196–216.
- Wang, X. and Dunson, D. B. (2013). Parallelizing MCMC via Weierstrass sampler. *arXiv preprint arXiv:1312.4605*.

- Welling, M. and Teh, Y. W. (2011). Bayesian learning via stochastic gradient Langevin dynamics. In *Proceedings of the 28th International Conference on Machine Learning*, pages 681–688.
- White, S., Kypraios, T., and Preston, S. (2015). Piecewise Approximate Bayesian Computation: fast inference for discretely observed Markov models using a factorised posterior distribution. *Statistics and Computing*, 25(2):289.
- Williamson, S. A., Dubey, A., and Xing, E. P. (2013). Parallel Markov chain Monte Carlo for nonparametric mixture models. In *Proceedings of the 30th International Conference on International Conference on Machine Learning*, pages 98–106.
- Zhang, Y., Wainwright, M. J., and Duchi, J. C. (2012). Communication-efficient algorithms for statistical optimization. In *Advances in Neural Information Processing Systems*, pages 1502–1510.
- Zhao, W., Ma, H., and He, Q. (2009). Parallel k-means clustering based on MapReduce. In *IEEE International Conference on Cloud Computing*, pages 674–679. Springer.
- Zuanetti, D. A., Müller, P., Zhu, Y., Yang, S., and Ji, Y. (2018). Bayesian nonparametric clustering for large data sets. *Statistics and Computing*, just accepted.